Intermediate in β-Lactam Hydrolysis Catalyzed by a Dinuclear Zinc(II) Complex: Relevance to the Mechanism of Metallo-β-lactamase

Natalia V. Kaminskaia, Bernhard Spingler, and Stephen J. Lippard*

Contribution from the Department of Chemistry, Massachusetts Institute of Technology, Cambridge, Massachusetts 02139

Received July 21, 2000

Abstract: Inactivation of β-lactam antibiotics by metallo-β-lactamase enzymes is a well-recognized pathway of antibiotic resistance in bacteria. As part of extensive mechanistic studies, the hydrolysis of a β-lactam substrate nitrocefin (**1**) catalyzed by dinuclear zinc(II) model complexes was investigated in nonaqueous solutions. The initial step involves monodentate coordination of the nitrocefin carboxylate group to the dizinc center. The coordinated substrate is then attacked intramolecularly by the bridging hydroxide to give a novel intermediate (**2′**) characterized by its prominent absorbance maximum at 640 nm, which affords a blue color. The NMR and IR spectroscopic data of **2′** are consistent with it being zinc(II)-bound N-deprotonated hydrolyzed nitrocefin that forms from the tetrahedral intermediate upon C−N bond cleavage. Protonation of the leaving group is the rate-limiting step in DMSO solution and occurs after the C−N bond-breaking step. Addition of strong acids results in rapid conversion of **2′** into hydrolyzed nitrocefin (**3**). The latter can be converted back to the blue species (**2′**) upon addition of base. The low pK_a value for the amino group in hydrolyzed nitrocefin is explained by its involvement in extended conjugation and by coordination to zinc(II). The blue intermediate (**2′**) in the model system resembles well that in the enzymatic system, judging by its optical properties. The greater stability of the intermediate in the model, however, allowed its characterization by ^{13}C NMR and infrared, as well as electronic, spectroscopy.

Introduction

β-Lactam antibiotics, such as penicillins and cephalosporins, contribute more than half of all the antibiotic drugs worldwide and once were called "superdrugs".[1] Unfortunately, because of the extensive and often unnecessary use of antibacterial agents, bacterial resistance to numerous antibiotics has spread so widely that some infections have become virtually untreatable.[1−3] Several pathways of bacterial resistance have been identified, including the expression of β-lactamases, enzymes that efficiently catalyze hydrolytic degradation of the β-lactam ring (eq 1), rendering antibiotics inactive.[4,5]

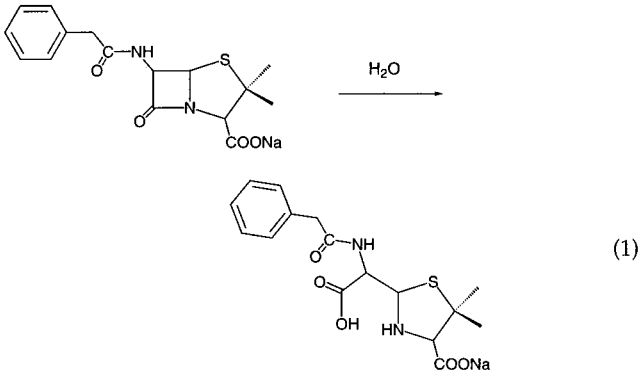

(1)

All β-lactamases can be divided into two main groups on the basis of their mechanism. The more abundant serine β-lactamases share an active-site serine residue that attacks the β-lactam carbonyl carbon to form an acyl−enzyme intermediate.[6] Mechanism-based suicide inhibitors, such as clavulanic acid or sulbactam, have been designed for serine β-lactamases and successfully used in therapy. Less common are metallo-β-lactamases, which require divalent zinc ions for catalytic activity.[6,7] These enzymes hydrolyze a wide range of substrates, including cephamycins and imipenem, that are resistant to the serine β-lactamases.[8,9] Moreover, the metallo-β-lactamases are not inactivated by traditional serine β-lactamase inhibitors, and at present there are no clinically useful inhibitors. Some metallo-β-lactamases are plasmid-encoded enzymes and can therefore be easily spread among various organisms.

Crystal structures have been reported for several metallo-β-lactamases.[10−13] Most enzymes are monomers composed of a single polypeptide chain[6] that is divided into two domains. The dizinc active site is located at the edge of a β-sheet sandwich

(1) Neu, H. C. *The Chemistry of β-Lactams*; Page, M. I., Ed.; Blackie: London, 1992; pp 101−128.
(2) Massova, I.; Mobashery, S. *Acc. Chem. Res.* **1997**, *30*, 162−168.
(3) Cohen, M. L. *Science* **1992**, *257*, 1050−1055.
(4) Hechler, U.; Van Den Weghe, M.; Martin, H. H.; Frère, J.-M. *J. Gen. Microbiol.* **1989**, *135*, 1275−1290.
(5) Frère, J.-M.; Dubus, A.; Galleni, M.; Matagne, A.; Amicosante, G. *Biochem. Soc. Trans.* **1999**, *27*, 58−63.
(6) Page, M. I.; Laws, A. P. *Chem. Commun.* **1998**, 1609−1617.
(7) Davies, R. B.; Abraham, E. P. *Biochem. J.* **1974**, *143*, 129−135.
(8) Bush, K. *Clin. Infect. Diseases* **1998**, *27*, S48−S53.
(9) Livermore, D. M. *J. Antimicrob. Chemother. Suppl. D* **1998**, *41*, 25−41.
(10) Concha, N. O.; Rasmussen, B. A.; Bush, K.; Herzberg, O. *Structure* **1996**, *4*, 823−836.
(11) Ullah, J. H.; Walsh, T. R.; Taylor, I. A.; Emery, D. C.; Verma, C. S.; Gamblin, S. J.; Spencer, J. *J. Mol. Biol.* **1998**, *284*, 125−136.
(12) Fabiane, S. M.; Sohi, M. K.; Wan, T.; Payne, D. J.; Bateson, J. H.; Mitchell, T.; Sutton, B. J. *Biochemistry* **1998**, *37*, 12404−12411.
(13) Carfi, A.; Pares, S.; Duée, E.; Galleni, M.; Duez, C.; Frère, J.-M.; Dideberg, O. *EMBO J.* **1995**, *14*, 4914−4921.

10.1021/ja002699e CCC: $20.00
Published on Web 06/16/2001

Scheme 1

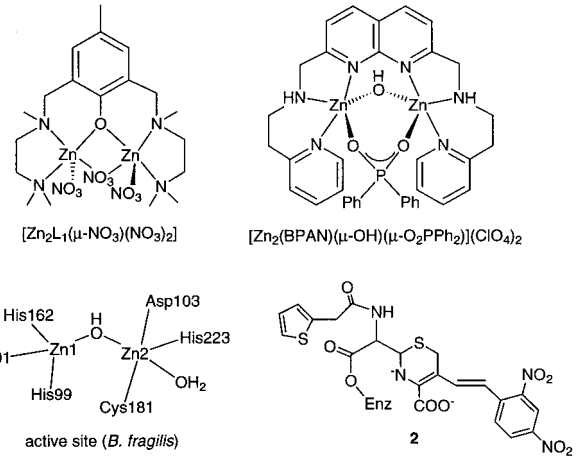

in the center of the molecule. The majority of metallo-β-lactamases have nearly identical dizinc-binding motifs that include a cysteine, an aspartate, and several histidine residues (Scheme 1). The two active-site zinc(II) ions are bridged by a hydroxide group in most metallo-β-lactamases. The enzymes all have either lysine or serine residues in the vicinity of the substrate binding site. Hydrogen bonding between these residues and the conserved carboxylate group in the β-lactam antibiotics is postulated to position the substrate favorably for hydrolysis at the active site.

There have been several studies of the mechanism of metallo-β-lactamase.[6,14−19] It is often proposed, with support from crystal structure determinations, that a zinc-bound hydroxide acts as the nucleophile to attack bound substrates.[15] At present, there is no definitive evidence about the exact position of the nucleophile during hydrolysis, namely, whether it resides in a terminal or bridging position at the dizinc(II) center. Dinuclear zinc(II) complexes developed as functional models of metallo-β-lactamases support a mechanism that involves a μ-OH^- unit as the active nucleophile.[20,21] Recently, an intermediate was detected by stopped-flow experiments in the hydrolysis of the β-lactam substrate nitrocefin **1** by the *Bacillus fragilis* enzyme.[14,16] UV−visible and kinetic data were consistent with a negatively charged species **2** (Scheme 1) that contains a deprotonated nitrogen atom as the leaving group. The detection of this intermediate suggested that cleavage of the C−N bond in β-lactam antibiotics occurs prior to protonation of the leaving group. This was the first such mechanistic proposal for the catalytic cycle of any zinc(II)-containing hydrolase. Although protonation of **2** was rate determining, the intermediate did not accumulate to a significant extent. Site-directed mutagenesis studies suggested that Asp-90 in β-lactamase from *Bacillus cereus* serves as a general acid and protonates the leaving group.[22] Despite the available UV−visible spectra for **2**, the structure of such a novel hydrolytic intermediate requires further investigation.

We recently reported the synthesis, structure, and reactivity of several functional β-lactamase models, including the two dizinc(II) complexes, $[Zn_2L_1(\mu\text{-}NO_3)(NO_3)_2]$ and $[Zn_2(BPAN)(\mu\text{-}OH)(\mu\text{-}O_2PPh_2)](ClO_4)_2$ (Scheme 1).[20,21] Monitoring β-lactam hydrolysis by these complexes in aqueous solution did not reveal any observable intermediates, presumably because the collapse of such species is more rapid than their formation.[20,21] Hydrolytic reactions carried out in wet DMSO as the solvent, however, resulted in the formation of a new species, the UV−visible spectrum of which was nearly identical to that of **2**.[21] We now report the spectroscopic and kinetic characterization of this intermediate, which is unprecedented among model systems for the metallo-β-lactamases.

Experimental Section

Chemicals. Starting materials and reagents $Zn(NO_3)_2\cdot 6H_2O$, $Zn(ClO_4)_2\cdot 6H_2O$, $Zn(OTf)_2$, $NaClO_4$, 2-(2-aminoethyl)pyridine, *N*,*N*,*N*′-trimethylethylenediamine, *p*-cresol, $NaBH_4$, 5-bromosalicylaldehyde, 2-amino-6-picoline, selenium dioxide, phosphorus oxychloride, ethyl acetoacetate, cyclen, and $(CH_3)_4NOH\cdot 5H_2O$ were obtained from Aldrich Chemical Co. Deuterated compounds D_2O, DMSO-d_6, acetone-d_6, chloroform-*d*, and dichloromethane-d_2 were purchased from Cambridge Isotope Laboratories. $LiOH\cdot H_2O$ and a 0.10 M standard solution of NaOH were obtained from Fluka. These and all other chemicals were of reagent grade. The hydrolytic substrate nitrocefin (2-(2,4-dinitrostyryl)-(6*R*,7*R*)-7-(2-thienylacetamide)-ceph-3-em-4-carboxylic acid, *E* isomer) **1** and a plasmid for metallo-β-lactamase from *B. fragilis* (CcrA) were kindly donated by Merck. The enzyme was purified by an unpublished procedure (J. H. Toney, Merck, Inc., private communication).

Physical Measurements. Proton and carbon-13 NMR spectra were obtained at 500 and 125 MHz, respectively, on Varian 500 and 501 NMR spectrometers equipped with temperature control units. HMQC $^1H-^{15}N$ NMR spectra were recorded on a Varian 500 spectrometer at 293 K, with *N*,*N*-dimethylformamide as an external reference. UV−visible spectra were recorded on a Cary 1E spectrophotometer equipped with a temperature controller. Solution IR spectra were obtained at room temperature on a Bio-Rad FTS-135 FTIR spectrometer between 400 and 4000 cm^{-1} using CaF_2 cells. The temperature was measured before and after each experiment, and the average value is reported.

Ligand Syntheses. Reactions were carried out under an atmosphere of dinitrogen or argon. The ligand HL_1 was synthesized according to a published procedure.[23] The neutral ligand was obtained as a colorless oil by treating the trihydrobromide salt with $NaHCO_3$. The precursor to the ligand 2,7-bis[2-(2-pyridylethyl)aminomethyl]-1,8-naphthyridine (BPAN), 2,7-dimethyl-1,8-naphthyridine, was synthesized from 6-methyl-2-pyridinamine and ethyl acetoacetate in four steps as described previously.[24] 1,8-Naphthyridine-2,7-dicarboxaldehyde was then synthesized from 2,7-dimethyl-1,8-naphthyridine by a modification of the published procedure.[25] Condensation of 1,8-naphthyridine-2,7-dicarboxaldehyde and 2-(2-aminoethyl)pyridine, followed by reduction with $NaBH_4$, gave ligand 2,7-bis[2-(2-pyridylethyl)aminomethyl]-1,8-naphthyridine (BPAN) as the final product.[25] The ligand *N*,*N*-bis(2-pyridylmethyl)-*tert*-butylamine (bpta) was prepared as described previously.[26]

Zinc Complexes. The complexes $[Zn_2L_1(\mu\text{-}NO_3)(NO_3)_2]$ and $[Zn_2(BPAN)(\mu\text{-}OH)(\mu\text{-}O_2PPh_2)](ClO_4)_2$ were synthesized according to

(14) Wang, Z.; Fast, W.; Benkovic, S. J. *Biochemistry* **1999**, *38*, 10013−10023.
(15) Wang, Z.; Benkovic, S. J. *J. Biol. Chem.* **1998**, *273*, 22402−22408.
(16) Wang, Z.; Fast, W.; Benkovic, S. J. *J. Am. Chem. Soc.* **1998**, *120*, 10788−10789.
(17) Walsh, T. R.; Gamblin, S.; Emery, D. C.; MacGowan, A. P.; Bennett, P. M. *J. Antimicrob. Chemother.* **1996**, *37*, 423−431.
(18) Paul-Soto, R.; Bauer, R.; Frère, J.-M.; Galleni, M.; Meyer-Klaucke, W.; Nolting, H.; Rossolini, G. M.; de Seny, D.; Hernandez-Valladares, M.; Zeppezauer, M.; Adolph, H.-W. *J. Biol. Chem.* **1999**, *274*, 13242−13249.
(19) Cricco, J. A.; Orellano, E. G.; Rasia, R. M.; Ceccarelli, E. A.; Vila, A. J. *Coord. Chem. Rev.* **1999**, *190−192*, 519−535.
(20) Kaminskaia, N. V.; He, C.; Lippard, S. J. *Inorg. Chem.* **2000**, *39*, 3365−3373.
(21) Kaminskaia, N. V.; Spingler, B.; Lippard, S. J. *J. Am. Chem. Soc.* **2000**, *122*, 6411−6422.
(22) Lim, H. M.; Iyer, R. K.; Pène, J. J. *Biochem. J.* **1991**, *276*, 401−404.
(23) Higuchi, C.; Sakiyama, H.; Okawa, H.; Fenton, D. E. *J. Chem. Soc., Dalton Trans.* **1995**, 4015−4020.
(24) Chandler, C. J.; Deady, L. W.; Reiss, J. A.; Tzimos, V. *J. Heterocycl. Chem.* **1982**, *19*, 1017−1019.
(25) He, C.; Lippard, S. J. *J. Am. Chem. Soc.* **2000**, *122*, 184−185.
(26) Mok, H. J.; Davis, J. A.; Pal, S.; Mandal, S. K.; Armstrong, W. H. *Inorg. Chim. Acta* **1997**, *263*, 385−394.

published procedures.[21,25] In the presence of water, the nitrate ligands in $[Zn_2L_1(\mu\text{-}NO_3)(NO_3)_2]$ are replaced with H_2O.[21,25]

Hydrolyzed Nitrocefin (3). This compound was prepared from nitrocefin following hydrolysis catalyzed by the metallo-β-lactamase from *B. fragilis*. In a typical experiment, nitrocefin (100 mg) was dissolved in 1.0 mL of DMSO and added stepwise to a solution of the enzyme (4.0 μM, 50 mL) in 50 mM MOPS buffer at pH 7. The mixture was incubated at room temperature for 1 h to ensure complete conversion to hydrolyzed nitrocefin. The pH of the solution was then adjusted to 3.3 with 4.0 N HCl, and the mixture was extracted twice (2 × 100 mL) with ethyl acetate. The extracts were combined and dried over $CaCl_2$, and the solvent was removed under vacuum to give the product (**3**). ^{1}H NMR in DMSO-d_6 for **3**: δ 8.70 d (J = 8.5 Hz, 1H, amide NH), 8.66 d (J = 2.5 Hz, 1H), 8.40 dd (J = 9.0 Hz, J = 2.0 Hz, 1H), 8.15 d (J = 15.5 Hz, 1H), 7.89 d (J = 8.5 Hz, 1H), 7.35 d (J = 5.0 Hz, 1H), 7.06 d (J = 5.5 Hz, 1H), 6.93 m (2H), 6.80 d (J = 15.5 Hz, 1H), 4.5 m (2H), 3.7 m (4H). ^{13}C NMR in DMSO-d_6 for **3** (carbonyl region): δ 170.3 (C(O)N), 169.4 (COO-lactamic), 165.1 (COO). ^{15}N NMR (obtained from HMQC experiments) in DMSO-d_6 for hydrolyzed nitrocefin: δ 120.0 (C(O)N), 91.0 (NH amine). HRMS ((FAB(+)) calcd for $C_{21}H_{18}N_4O_9S_2$, 535.0594; found, 535.0578(17). Anal. Calcd for $C_{21}H_{18}N_4O_9S_2\cdot 2$DMSO: C, 43.47; H, 4.38; N, 8.11. Found: C, 43.12; H, 4.47; N, 7.87.

Decomposition. The decomposition of nitrocefin (**1**) and hydrolyzed nitrocefin (**3**) is accompanied by the loss of visible absorbance.[27,28] The major decomposition products were characterized by UV−visible spectrophotometry and by their ^{1}H, ^{13}C, and HMQC NMR spectra in DMSO-d_6 solution. ^{1}H NMR in DMSO-d_6 for decomposed **1** (major product): δ 9.25 d (J = 8.5 Hz, 1H, amide NH), 8.75 d (J = 3.5 Hz, 1H), 8.50 dd (J = 15.0 Hz, J = 3.5 Hz, 1H), 8.00 d (J = 10.0 Hz, 1H), 7.40 m (1H), 6.93 m (2H), 5.80 m (1H), 5.56 m (1H, C10−H), 5.24 d (1H, J = 10 Hz), 4.0 m (4H), 3.3 m (2H, C9−H). ^{13}C NMR in DMSO-d_6 for decomposed **1** (major product): δ 170.0 (amide), 165.0, 164.0, 149.3, 146.1, 143.3, 143.0, 137.1, 137.0, 136.5, 134.5, 128.5, 127.5, 124.0, 120.5, 81.6 and 81.5 (C10), 59.8 and 57.3, 35.0 (C9), 22.0. ^{13}C resonances at 81.6 and 81.5 ppm correlate with ^{1}H resonances at 5.56 ppm. ^{13}C resonance at 35.0 correlates with ^{1}H resonances at 3.30 ppm. ^{1}H NMR in DMSO-d_6 for decomposed **3** (major product): δ 8.73 m (1H), 8.62 d (J = 15 Hz, 1H), 8.52 d (J = 12.5 Hz, 1H), 7.90 d (J = 12.5 Hz, 1H), 7.35 m (1H), 6.94 m (2H), 6.0 dd (J = 100 Hz, J = 10 Hz, 1H), 5.30 m (1H, C10−H), 4.80 m (2H), 3.70 m (4H), 3.15 m (2H, C9−H). ^{13}C NMR (HMQC) in DMSO-d_6 for decomposed **3** (major product): δ 135.0, 128.3, 128.0, 127.0, 126.0, 125.1, 121.5, 121.0, 81.9 (C10), 58.0 and 56.0, 35.8 (C9), 25.8. ^{13}C resonance at 81.9 ppm correlates with ^{1}H resonances at 5.30 ppm. ^{13}C resonance at 35.9 ppm correlates with ^{1}H resonances at 3.15 ppm. These data are consistent with hydration of the C9−C10 double bond to yield the respective 10-hydroxyl derivatives as the decomposition products. The decomposition of the blue species (**2′**) without added acid is also accompanied by loss of visible absorbance. It was therefore concluded that hydration of the C9−C10 double bond is the main cause for the decomposition of **2′** in the absence of acid. In the presence of acid, **3** was the only decomposition product observed.

Binding of β-Lactam Substrates to Zn(II) Compounds in DMSO Solution. (i) Carbon-13 NMR Experiments. In the data reported below, chemical shifts are given in ppm relative to DMSO-d_6 as an internal reference. In a typical experiment, the solution was initially 0.10 M in complex and 0.10 M in nitrocefin. The temperature was 293 K, unless stated otherwise. ^{13}C NMR in DMSO-d_6 for free nitrocefin (carbonyl region): δ 169.5 (C(O)N), 164.0 (COO), 162.4 (C(O)N-lactam). ^{13}C NMR in a 1:1 mixture of DMSO-d_6 and acetone-d_6 for free nitrocefin (carbonyl region): δ 170.5 (C(O)N), 165.1(COO), 163.6 (C(O)N-lactam). ^{13}C NMR in a 1:1 mixture of DMSO-d_6 and acetone-d_6 for nitrocefin in the presence of $[Zn_2L_1(\mu\text{-}NO_3)(NO_3)_2]$ (carbonyl region): δ 170.6 (C(O)N), 168.8 and 168.0 (COO), 165.3 (C(O)N-lactam). ^{13}C NMR in DMSO-d_6 for nitrocefin in the presence of $[Zn_2L_1(\mu\text{-}NO_3)(NO_3)_2]$ (carbonyl region): δ 170.5 (C(O)N), 168.4 and 167.4 (COO), 165.0 and 164.5 (C(O)N-lactam). ^{13}C NMR in DMSO-d_6 at 313 K for nitrocefin in the presence of $[Zn_2L_1(\mu\text{-}NO_3)(NO_3)_2]$ (carbonyl region): δ 170.4 (C(O)N), 168.3 and 167.5 (COO), 164.8 and 164.5 (C(O)N-lactam).

(ii) ^{1}H−^{15}N HMQC Experiments. In a typical experiment, the solution was initially 0.10 M in complex and 0.10 M in nitrocefin. The temperature was 293 K. ^{15}N NMR in DMSO-d_6 for nitrocefin: δ 109.6 (C(O)N). ^{15}N NMR in DMSO-d_6 for nitrocefin in the presence of $[Zn_2L_1(\mu\text{-}NO_3)(NO_3)_2]$: δ 109.5 (C(O)N). The ^{1}H and ^{15}N chemical shifts are given in ppm relative to DMSO-d_6 as an internal reference and to dimethylformamide as an external reference, respectively.

(iii) Infrared Experiments. The initial concentrations of complex and nitrocefin were each 0.05 M, and the solvent was always DMSO. The temperature was 293 K. Typical spectra were recorded within 1 min after mixing the reagents. IR (cm^{-1}) for free nitrocefin (carbonyl region): 1700 br (ν_{asym}(COO)), 1684 (C(O)N), 1781 (C(O)-lactam). IR (cm^{-1}) for nitrocefin in the presence of $[Zn_2L_1(\mu\text{-}NO_3)(NO_3)_2]$ (carbonyl region): 1634 (ν_{asym}(COO)), 1680 br (C(O)N), 1783 (C(O)-lactam).

Synthesis of the Blue Species (2′) for Spectroscopic Experiments. (i) NMR Experiments. (A) The complex $[Zn_2L_1(\mu\text{-}NO_3)(NO_3)_2]$ (2.1 × 10^{-4} mol, 127.4 mg) and nitrocefin (2.1 × 10^{-4} mol, 108.0 mg) were mixed in 0.35 mL of DMSO-d_6, and 0.35 mL of acetone-d_6 was added. Two equivalents of LiOH·H_2O (4.2 × 10^{-4} mol, 17.6 mg), dissolved in a minimal amount of D_2O (50 μL), was added to the reaction mixture, which was then incubated at 313 K for 8 h. The initial concentrations of nitrocefin and the complex were each 0.28 M. The concentrations of the blue species and nitrocefin were monitored by UV−visible spectrophotometry during the incubation. When conversion of nitrocefin to the blue species was 50% complete, the incubation was stopped and the ^{13}C NMR spectrum of the sample recorded at 293 K. Similar experiments were performed with 1 equiv of LiOH·H_2O (2.1 × 10^{-4} mol, 8.8 mg) present in the reaction mixture. ^{13}C NMR spectra in a 1:1 mixture of acetone-d_6 and DMSO-d_6 at 293 K of **2′** in the presence of $[Zn_2L_1(\mu\text{-}NO_3)(NO_3)_2]$ (carbonyl region): δ 170.6 (C(O)N), 170.0 (COO), 171.5 (COO-lactamic).

(B) The $[Zn_2L_1(\mu\text{-}NO_3)(NO_3)_2]$ complex (8.0 × 10^{-5} mol, 52.0 mg) and hydrolyzed nitrocefin **3** (8.0 × 10^{-5} mol, 42.7 mg) were each dissolved in 0.40 mL of DMSO-d_6, and the two solutions were then mixed at room temperature. The concentration of the blue species was monitored by UV−visible spectrophotometry. ^{13}C NMR in DMSO-d_6 at 293 K of **3** in the presence of $[Zn_2L_1(\mu\text{-}NO_3)(NO_3)_2]$ (carbonyl region): δ 169.4 (C(O)N), 169.3 (COO), 174.0 (COO-lactamic). ^{1}H NMR in DMSO-d_6 for **3** in the presence of $[Zn_2L_1(\mu\text{-}NO_3)(NO_3)_2]$: δ 8.60 br, 8.50 br, 8.25 br, 7.75 br, 7.30 br, 6.90 br, 6.80 br, 6.55 br, 4.80 br, 4.0 br, 3.70 br, 3.20 br, 2.80 br, 2.60 br, 2.20 br. The β-lactam N−H proton is not visible. A ^{1}H−^{15}N HMQC experiment did not yield reliable signals due to exchange processes.

(ii) Infrared Experiments. The $[Zn_2L_1(\mu\text{-}NO_3)(NO_3)_2]$ (2.5 × 10^{-5} mol, 15.2 mg) complex and nitrocefin (2.5 × 10^{-5} mol, 13.0 mg) were dissolved in 0.50 mL of DMSO, and 2 equiv of LiOH·H_2O (5.0 × 10^{-5} mol, 2.1 mg) in 10 μL of H_2O was added. The reaction mixture was incubated at 313 K for 8 h. The initial concentrations of nitrocefin and the complex were each 0.05 M. The time-dependent relative concentrations of nitrocefin and the blue species were determined from the UV−visible spectra during the incubation. When 80% of the nitrocefin had converted to the blue species, the incubation was stopped and IR spectra were recorded.

Extinction Coefficients of Nitrocefin and 2′. The extinction coefficient (ε) of nitrocefin at 390 nm is 21 000 M^{-1} cm^{-1} in HEPES buffer at 313 K.[21] The value of ε (400 nm) in a DMSO solution containing 0.05 M H_2O at 333 K was 18 800 M^{-1} cm^{-1} and was unaffected by the presence of zinc(II) complexes or salts (Figure S1). This ε value was unaltered over the temperature range 293−333 K.

The extinction coefficient for the blue species (**2′**) was determined during the course of its conversion from nitrocefin. In a typical experiment, the zinc complex and nitrocefin were mixed in DMSO, and the reaction mixture was heated in the temperature-controlled compartment of the UV−visible spectrophotometer. Consumption of nitrocefin and formation of **2′** were followed at 400 and 640 nm, respectively, and the absorbances of the two compounds at each time

(27) O'Callaghan, C. H. *Antimicrob. Agents Chemother.* **1978**, *13*, 628−633.

(28) O'Callaghan, C. H.; Morris, A.; Kirby, S. M.; Shingler, A. H. *Antimicrob. Agents Chemother.* **1972**, *1*, 283−288.

Table 1. Effect of Weak and Strong Acids on the Formation and Disappearance of the Blue Species at 333 K[a]

acid	pK_a	k_{form}, min^{-1}	k_{dis}, min^{-1}
none		0.20	0.005
trifluoroacetic acid[b]	<0	n.r.[c]	>200[d]
acetic acid[b]	4.75	n.r.[c]	>200[d]
pyridinium triflate	5.10	n.r.[c]	>200[d,e]
2-chloro-4-nitrophenol	5.45	n.r.[c]	0.006[d]
2,4,6-trichlorophenol	5.99	n.r.[c]	0.004[d]
4-chloro-2-nitrophenol	6.46	n.r.[c]	0.004[d]
2,6-dibromophenol	6.67	n.r.[c]	0.003[d]
2,6-dichlorophenol	6.79	n.r.[c]	0.003[d]
p-nitrophenol[b]	7.16	0.25	0.004[d]
trifluoroethanol[b]	12.4	0.23	0.004[d]
H_2O[b]	15.9	0.17	0.009[d]

[a] The solvent was neat DMSO that was made 1.11 M in H_2O; initial concentrations of nitrocefin and complex were 3.8×10^{-5} and 5.0×10^{-4} M, respectively. [b] The respective concentrations of trifluoroacetic and acetic acids, *p*-nitrophenol, trifluoroethanol, and H_2O were 0.01, 0.08, 0.01, 0.073, and 0.28 M. The concentrations of 2-chloro-4-nitrophenol, 2,4,6-trichlorophenol, 4-chloro-2-nitrophenol, 2,6-dibromophenol, 2,6-dichlorophenol, and pyridinium triflate were 2.0×10^{-4} M each. [c] No reaction, if the acid is present in the solution of nitrocefin and $[Zn_2L_1(\mu\text{-}NO_3)(NO_3)_2]$. [d] Each acid was added to the preformed **2′** and the k_{dis} values were measured. [e] Addition of 0.001 M pyridine to the 5.0×10^{-5} M solution of **2′** did not result in the decomposition of **2′**.

point were recorded. The ϵ value of 38 900 M^{-1} cm^{-1} was then determined from the resulting Beer's law plot (Figure S2). It was independent of temperature between 293 and 333 K.

Determination of the pK_a Value of 2′. Pyridinium triflate was used as the acid in protonation equilibrium studies of **2′**. In a typical experiment, various concentrations (5.0×10^{-5}–5.0×10^{-4} M) of pyridinium triflate were added to a 5.0×10^{-5} M solution of preformed **2′** in DMSO, and the resulting solution was allowed to equilibrate for 5 min at 293 K. The concentrations of **2′** and **3** after each addition were determined by UV−visible spectroscopy. The respective equilibrium concentrations of pyridinium triflate and pyridine (py) were then calculated on the basis of the known total concentrations. The values of $K_{eq} = ([\mathbf{3}][py])/([pyH^+][\mathbf{2'}])$ were computed for each addition of the acid. The acid dissociation constant of **2′** (K_a) was determined from the expression $K_a = K_a'/K_{eq}$, where K_a' is the acid dissociation constant of pyH^+ (7.94×10^{-6}). Pyridine itself does not influence the decomposition of **2′** (Table 1).

Ruling Out the DMSO Anion as the Blue Species. Sodium hydride and DMSO were stirred at 343 K for 1 h to afford a pale yellow-green solution of the sodium salt of dimethyl sulfoxide anion.[29] Addition of various bases, including LiOH, NaOMe, NaO^{t}Bu, and lithium diisopropylamide (LDA), to DMSO solutions under our experimental conditions produced colorless to yellow solutions. The blue species did not form in DMSO solution in the absence of nitrocefin. Relatively weak acids, such as *p*-nitrophenol, water, and trifluoroethanol, do not quench the blue species. Therefore, the blue color that forms in the presence of nitrocefin does not arise from the DMSO anion.

Synthesis of the Blue Species in the Absence of Zinc(II) Compounds. The initial concentrations of nitrocefin and $(CH_3)_4NOH\cdot 5H_2O$ used in these experiments were either each 5.0×10^{-5} M, or 5.0×10^{-5} and 2.5×10^{-4} M, respectively. The solvent was DMSO made 0.05 M in H_2O, and the temperature was 333 K. Dry DMSO solutions were prepared by stirring them overnight above 4 Å activated molecular sieves.

Kinetics of the Hydrolysis Reaction. The kinetics was followed by UV−visible spectrophotometry. The temperature inside the UV−visible cuvettes was measured directly with a thermocouple. The solvent was DMSO. Unless stated otherwise, the concentration of water in DMSO solutions was determined by ^{1}H NMR spectroscopy to be 0.05 M. The substrate used for the kinetic studies was nitrocefin, **1**. The product, hydrolyzed nitrocefin, absorbs at 496 nm ($\epsilon_{496} = 16\,000$ M^{-1} cm^{-1}). Stock solutions of the complexes and nitrocefin were prepared in DMSO and used immediately to avoid decomposition. Their concentrations were 0.010 M each. Unless stated otherwise, the concentrations of $[Zn_2L_1(\mu\text{-}NO_3)(NO_3)_2]$ and nitrocefin in kinetic studies were 4.7×10^{-4} and 3.7×10^{-5} M, respectively.

Scheme 2

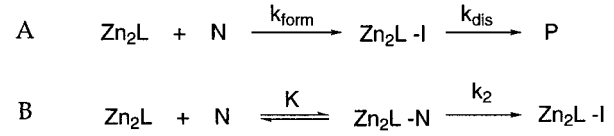

In a typical kinetic run, all reagents were mixed in a spectrophotometric cell and allowed to equilibrate for 2 min inside the temperature-controlled UV−visible spectrophotometer compartment before data collection was begun. Data were usually collected at 640 nm, the wavelength that corresponds to the absorbance maximum of **2′** in the presence of $[Zn_2L_1(\mu\text{-}NO_3)(NO_3)_2]$. A representative trace, collected at 640 nm, is shown in Figure S3. Nitrocefin and its hydrolysis product do not absorb around 600−700 nm. Consequently, their spectra do not interfere with the kinetic data, revealing the formation and disappearance of the blue species (**2′**). The rate constants for the formation of the blue species (**2′**) were determined by fitting the experimental dependence on the concentration of **2′** at different times to eq 2 to account for the loss in absorbance with time owing to decomposition. The formation and decomposition steps were irreversible under the experimental conditions. In eq 2, k_{form} and k_{dis} are the rate constants for the

$$Abs_t = \frac{\epsilon_1 k_{form}[N]_0}{k_{dis} - k_{form}} [\exp(-k_{form}t) - \exp(-k_{dis}t)] \qquad (2)$$

formation and disappearance of the intermediate (Scheme 2A), respectively. Typically, the concentration of water in DMSO was kept sufficiently high (>0.05 M) to ensure complete displacement of NO_3^- ligands in $[Zn_2L_1(\mu\text{-}NO_3)(NO_3)_2]$. Thus, in experiments concerning the pK_a value of **2′**, the concentration of water was 1.1 M.

In the experiments investigating the effect of $[Zn_2L_1(\mu\text{-}NO_3)(NO_3)_2]$ on the formation of **2′**, the initial concentration of nitrocefin was 3.8×10^{-5} M, and the concentration of the complex was varied. In experiments evaluating the stability of **2′**, 0.06 M sodium acetate, 0.005 M 1-methylimidazole, and 0.01 M bpta were added sequentially to a solution containing 3.7×10^{-5} M **2′**. The decomposition of **2′** was followed by UV−visible spectrophotometry after each sequential addition.

Results and Discussion

Binding of β-Lactam Substrates to Zn(II) Compounds in DMSO Solution. Data in this and the previous reports[20,21] demonstrate that the ^{13}C NMR and infrared spectroscopic methods are well suited to monitor coordination of β-lactam substrates to dinuclear and mononuclear zinc(II) complexes in DMSO solutions. A downfield shift of the carboxylic acid carbonyl resonance (Experimental Section) upon addition of $[Zn_2L_1(\mu\text{-}NO_3)(NO_3)_2]$ to nitrocefin (**1**) is a clear indication that the carboxylate group binds to zinc(II).[30] The blue shift and position of ν_{asym}(COO) are also consistent with monodentate carboxylate binding to a zinc(II) ion.[31−33] These spectral changes are clearly due to complexation of nitrocefin rather than simple deprotonation of **1** by the zinc(II) complex. The latter would result in a ν_{asym}(COO) stretch at ca. 1600 cm^{-1}. The small changes in the chemical shift and in the ν(C(O)-β-lactam) stretching frequency presumably result from inductive effects

(29) Corey, E. J.; Chaykovsky, M. *J. Am. Chem. Soc.* **1965**, *87*, 1345−1353.

(30) Kaminskaia, N. V.; Kostić, N. M. *Inorg. Chem.* **1997**, *36*, 5917−5926.

(31) Ferrer, E. G.; Williams, P. A. M. *Polyhedron* **1997**, *16*, 3323−3325.

(32) Kupka, T. *Spectrochim. Acta Part A* **1997**, *53*, 2649−2658.

(33) Zevaco, T. A.; Görls, H.; Dinjus, E. *Polyhedron* **1998**, *17*, 2199−2206.

that originate from zinc(II) coordination to the carboxylate group.[32,34] The two carboxylate group carbon resonances in the ^{13}C NMR spectra of bound nitrocefin in DMSO-d_6 presumably correspond to two rotational isomers. The respective resonances in two pairs broaden and partially coalesce in a 1:1 mixture of acetone and DMSO, which has a lower solvent viscosity.[35] Increasing the temperature to 313 K also results in such partial coalescence. That this result is not a consequence of different modes of nitrocefin binding was ruled out by IR experiments that reveal only monodentate coordination of the carboxylate group. Penicillin G also binds to dinuclear and mononuclear zinc(II) complexes via the carboxylate group in a monodentate manner according to the ^{13}C and IR data.[21] Thus, variations in structure among cephalosporins, such as cephalothin and nitrocefin, and penicillins do not affect the mode of metal binding. The rate constant for nitrocefin binding is >3 min^{-1} at 293 K. Addition of equimolar Cl^- or a 10-fold molar excess of CH_3COO^- to the 0.05 M solution of $[Zn_2L_1(\beta\text{-lactam})]^{2+}$, where β-lactam is nitrocefin or penicillin G, results in rapid dissociation of the β-lactam substrate, as evidenced by IR spectroscopy. The dissociation rate constant is greater than 5 min^{-1} at 293 K. Therefore, binding of the β-lactam substrates is fast and reversible. No hydrolysis of the β-lactam substrates was observed in these binding experiments.

Hydrolysis of β-Lactam Substrates Catalyzed by the Dinuclear Zinc(II) Complexes. Nitrocefin (**1**) was chosen as a substrate to investigate hydrolysis because it conveniently absorbs in the visible region at 400 nm. This visible absorbance maximum shifts to 496 nm upon hydrolysis owing to formation of **3**, as indicated in eq 3. Previously reported mechanisms for

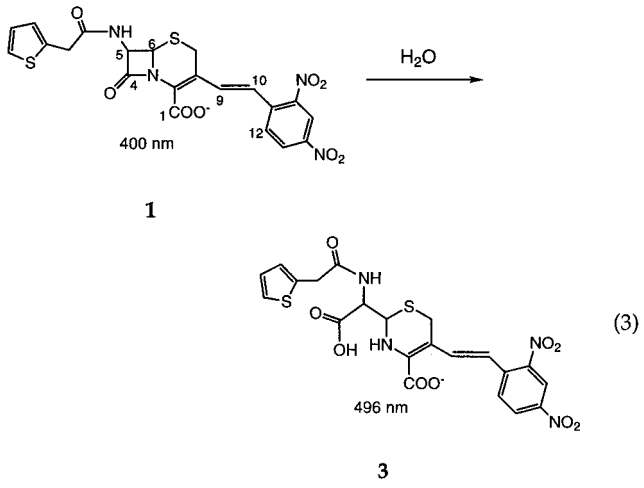

(3)

β-lactam hydrolysis by the complexes $[Zn_2L_1(\mu\text{-OH})(NO_3)_2]$ and $[Zn_2(BPAN)(\mu\text{-OH})(\mu\text{-}O_2PPh_2)](ClO_4)_2$ are provided in Schemes S1 and S2.[20,21] Both complexes bind β-lactam substrates as monodentate ligands via the conserved carboxylate group. The nature of the reactive species in the two cases is different, however. The bridging hydroxide in $[Zn_2L_1(\mu\text{-OH})(\text{substrate})(H_2O)]^+$ acts as the reactive species because it is conveniently positioned cis to the coordinated substrate and because its lability and nucleophilicity are increased in the presence of the negatively charged phenolate ligand. Unfavorable trans positioning of the bridging hydroxide with respect to the bound substrate and the higher positive charge in $[Zn_2(BPAN)(\mu\text{-OH})(\text{substrate})(OH_2)]^{2+}$ result in deactivation of the hydroxide bridge.[20,21] A terminal hydroxide formed upon dissociation of diphenylphosphinate serves as the nucleophile that attacks coordinated substrates. Nucleophilic attack by the bridging or terminal hydroxide is the rate-determining step in hydrolysis by both complexes in aqueous solution.

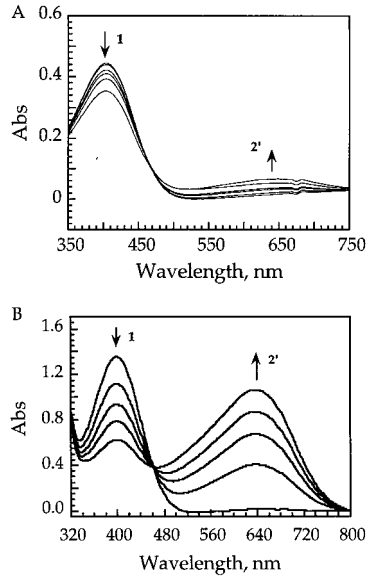

Figure 1. Hydrolysis of nitrocefin in DMSO followed by UV−visible spectroscopic experiments in the presence of $[Zn_2L_1(\mu\text{-}NO_3)(NO_3)_2]$. The initial concentration of the complex was 4.7×10^{-4} M. (A) The temperature and initial concentration of nitrocefin were 296 K and 3.8×10^{-5} M. The spectra were recorded during the first hour after mixing (after 7, 20, 27, 50, 65 min). (B) The temperature and initial concentration of nitrocefin were 333 K and 3.8×10^{-5} M. The spectra were recorded every 8 min (B).

Fast C−N bond cleavage and protonation of the leaving group to afford product made it impossible to observe the intermediate in aqueous solution at pH 7. We considered that significant buildup of an anionic intermediate that is similar to **2** might take place at higher pH values where the rate of protonation would be retarded. No accumulation of an intermediate was observed, however, when the reaction was followed by UV−visible spectroscopy at pH 8.59 at either 296 (Figure S4) or 313 K. Presumably, the protonation step is sufficiently rapid under these conditions that the intermediate decomposes more rapidly than it forms. Raising the solution pH to values higher than 8.59 resulted in decomposition of nitrocefin.

Formation of the Intermediate in DMSO Solutions of Nitrocefin. Reaction of nitrocefin with a 10-fold molar excess of $[Zn_2L_1(\mu\text{-}NO_3)(NO_3)_2]$ at room temperature in wet DMSO solution resulted in formation of a new species (**2′**) having an absorbance maximum at 640 nm (Figure 1A). At 333 K, **2′** is formed in higher concentrations (Figure 1B). This new species also appears in the presence of only 1 equiv of the zinc(II) complex (Figure S5). Because of similarities between the absorption spectra of **2′** in the model system and **2** in the enzyme, we conclude that the blue species obtained in the presence of $[Zn_2L_1(\mu\text{-}NO_3)(NO_3)_2]$ and metallo-β-lactamase have similar structures.

Effects of pH on the Blue Species. Addition of a strong organic acid, such as CF_3COOH, to a solution of the blue zinc complex in DMSO resulted in an instantaneous color change to pink (Figure 2). A new band at 496 nm arises from the product of nitrocefin hydrolysis, **3**. Thus, the blue species is a true intermediate on the pathway from nitrocefin (**1**) to hydrolyzed nitrocefin (**3**), and not a side product. Further

(34) Anacona, J. R.; Figueroa, E. M. *J. Coord. Chem.* **1999**, *48*, 181−189.

(35) *CRC Handbook of Chemistry and Physics*; CRC Press: Boca Raton, FL, 1991−1992.

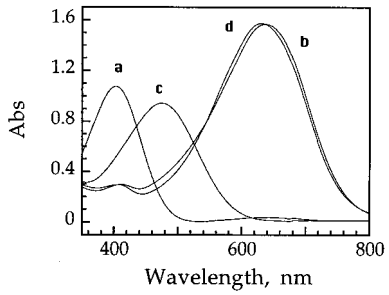

Figure 2. UV−visible spectra that reflect the interconversion of nitrocefin and the blue species in DMSO: (a) nitrocefin; (b) blue species formed upon heating at 333 K in the presence of 4.7×10^{-4} M [Zn_2L_1-(μ-NO_3)(NO_3)$_2$]; (c) hydrolyzed nitrocefin formed upon addition of 2.0×10^{-3} M trifluoroacetic acid to the solution of the blue species in (b); (d) blue species reformed upon the addition of 4×10^{-3} M $(CH_3)_4$-NOH·H_2O to the solution of hydrolyzed nitrocefin in (c).

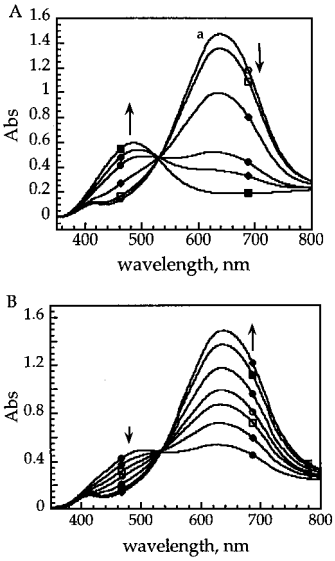

Figure 3. (A) Quenching **2′** by stepwise addition of CF_3COOH at 293 K. Mixing hydrolyzed nitrocefin (3.8×10^{-5} M) and [Zn_2L_1-(μ-NO_3)(NO_3)$_2$] (5.0×10^{-5} M) produces **2′** (○, spectrum a); 0.01 M CF_3COOH is added stepwise (□, 5.0×10^{-6} M; ◇, 1.5×10^{-5} M; ●, 3.0×10^{-5} M; ◆, 3.5×10^{-5} M; ■, 4.0×10^{-5} M) to achieve a final concentration of 4.0×10^{-5} M. (B) Reforming **2′** by stepwise addition of 0.01 M $(CH_3)_4NOH$ to achieve a final concentration of 4.0×10^{-5} M. The temperature was 293 K.

addition of base (Figure 2) restored the blue color of the intermediate (**2′**). The interconversion between blue species (**2′**) and hydrolyzed nitrocefin (**3**) is therefore reversible and affected solely by pH. This finding is consistent with a deprotonated amine structure, similar to that of **2**, for the blue zinc complex.

Preparation of 2′ from Hydrolyzed Nitrocefin (3). The blue species (**2′**) can be prepared directly from **3**, as described in the Experimental Section. Its UV−visible spectrum (Figure 3A) is identical to that of material prepared from nitrocefin **1** (Figure 2). Stepwise addition of acid results in protonation of the amine group in **2′** and subsequent conversion of **2′** to **3**, as the results in Figure 3A show. The blue color disappears only when the amine group is protonated. Neutralization with base leads to the reappearance of **2′** (Figure 3B).

Spectroscopic Characterization of 2′. Samples for ^{13}C NMR and IR experiments were prepared as described in the Experimental Section. Several changes are evident in the ^{13}C NMR spectra of bound nitrocefin upon heating. Most notably, the β-lactam resonance at 165.3 ppm disappears and is replaced by a new resonance at 171.5 ppm. The position of the latter resonance is the same as that appearing when the β-lactam is hydrolyzed upon heating in the presence of the dizinc(II) complex. The carboxylate resonances of bound nitrocefin at 168.8 and 168.0 ppm shift downfield to afford a broad feature at 170 ppm. The amide resonance at 170.6 ppm does not shift significantly. These spectroscopic features are consistent with structure **2′** for the blue intermediate. Similar spectroscopic results were obtained when **2′** was prepared directly from hydrolyzed nitrocefin **3** (Experimental Section).

The results of the IR experiments support this conclusion. The stretching frequency of the β-lactam carbonyl group at 1781 cm^{-1} disappears upon heating, and a new feature at 1673 cm^{-1} appears. The position of this new band is consistent with hydrolysis of the β-lactam group in nitrocefin and binding of the newly formed carboxylate to the dizinc(II) complex. These changes were observed only in the subtracted spectra because the amide and two carboxylate carbonyl bands overlap one another between 1600 and 1700 cm^{-1}. The structure postulated for **2′** on the basis of these experiments is depicted below.

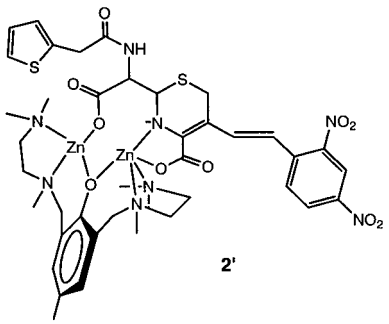

The blue color of the intermediate arises from extended conjugation that involves the deprotonated amine nitrogen atom.[14,16] Protonation of the two carboxylate groups in **1** and **3** does not affect the visible spectrum significantly.

Effect of Weak and Strong Acids on the Formation and Disappearance of the Blue Species. Hydrolysis of nitrocefin is inhibited at low pH values in aqueous solutions because the concentration of the active Zn_2−OH species is low.[21] The pH value of DMSO solutions used in the present study could not be quantitated. Instead, various acids were added to the reaction mixture, and their effects on k_{form} and k_{dis} (eq 2) were determined. Table 1 lists the respective observed rate constants together with the pK_a values of the various acids. Only CH_3COOH, CF_3COOH, and pyridinium triflate significantly affect the formation and disappearance rate constants. In the presence of acids having pK_a values lower than that of Zn_2−OH_2, k_{form} decreases to an undetectable level because the concentration of the reactive species Zn_2−OH is drastically diminished. Addition of several acids to preformed **2′** affords increased k_{dis} values (Table 1) because **2′** is protonated and converted to **3**. This finding is consistent with a pK_a value lower than 5.45 for protonation of the blue species. The deprotonated nitrogen atom is most likely bound to a zinc(II) ion in **2′** to maintain such a low pK_a value. A more precise pK_a value for **2′** was obtained from the equilibrium study that employed pyridinium triflate as the acid to protonate this species (Experimental Section). These experiments yielded a pK_a value of 4.2 for protonation of the amine nitrogen atom in **2′**. Addition of the excess acetic acid, which has a higher pK_a value, results in complete conversion of **2′** to **3** (Table 1).

Effect of [Zn_2L_1(μ-NO_3)(NO_3)$_2$] on Formation of the Blue Species. Increasing the concentration of the complex resulted

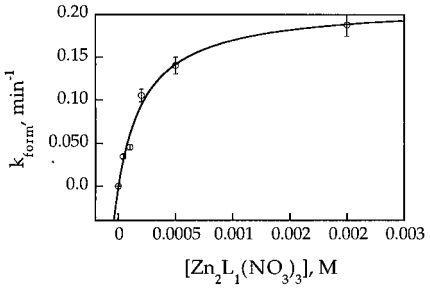

Figure 4. Effect of $[Zn_2L_1(\mu\text{-}NO_3)(NO_3)_2]$ on formation of the blue species. The initial concentration of nitrocefin was 3.8×10^{-5} M, the solvent was DMSO, and the temperature was 333 K. The concentration of water was 0.328 M.

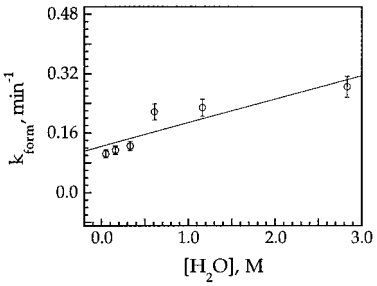

Figure 5. Effect of water on the formation of the blue species in the presence of $[Zn_2L_1(\mu\text{-}NO_3)(NO_3)_2]$. The initial concentrations of nitrocefin and the complex were 3.8×10^{-5} and 2.0×10^{-3} M, the solvent was DMSO, and the temperature was 333 K. The line is drawn to guide the eye.

in more rapid formation of 2′, as the data in Figure 4 show. The saturation behavior arises from binding of nitrocefin to the dizinc(II) complex prior to conversion to **2′**, as drawn in Scheme 2B. The experimental results in Figure 4 were fit to eq 4 to

$$k_{form} = \frac{Kk_2[Zn_2L]_0}{K[Zn_2L]_0 + 1} \quad (4)$$

obtain equilibrium and rate constants of 3980 ± 730 M^{-1} and 0.21 min^{-1}, respectively. Notably, the disappearance of nitrocefin exhibits similar saturation kinetics.[21] The value of K in DMSO solution is lower than that in a 1:9 mixture of DMSO and acetone, presumably because DMSO competes better than acetone with nitrocefin for binding to the dizinc(II) complex.[21]

Effect of Water Concentration on the Conversion of Nitrocefin to the Blue Species. The nitrocefin binding constant (K) is dependent on water concentration because water and the β-lactam substrate compete for coordination.[21] Thus, increasing $[H_2O]$ 10 times (from 0.112 to 1.112 M) lowers the K value from 3.1×10^4 to 1.7×10^4 M^{-1} in a 1:9 mixture of DMSO and acetone. Addition of high, saturating concentrations of the dizinc complex ($>1 \times 10^{-3}$ M) ensures complete binding of the β-lactam substrate in the presence of 0.328 M water (Figure 4). The values of k_{form} were determined under the aforementioned saturating conditions, when nearly all nitrocefin is bound, and plotted against water concentration, as shown in Figure 5. Notably, k_{form} values slightly increase with $[H_2O]$, but the changes are relatively small. Closer examination of the graph at water concentrations below 2.0 M gives approximately 0.2 order of the reaction with respect to $[H_2O]$. Nearly zeroth order on water concentration indicates an internal attack mechanism (Scheme S1). An external attack mechanism would result in clear first-order kinetics.[21]

Temperature Effects. The formation of **2′** obeys a linear Eyring relationship, as shown in Figure 6. The rate constant

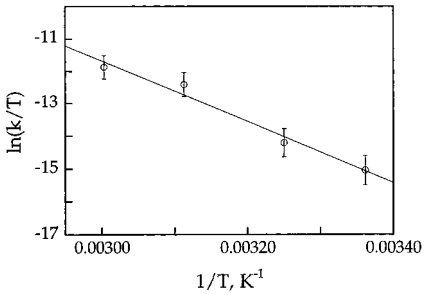

Figure 6. Effect of temperature on the formation of the blue species in the presence of $[Zn_2L_1(\mu\text{-}NO_3)(NO_3)_2]$. The initial concentrations of nitrocefin and the complex were 3.8×10^{-5} and 2.0×10^{-4} M, and the solvent was DMSO. The concentration of water was 0.328 M.

k_{form} in DMSO is a microscopic rate constant that corresponds to the hydrolysis of coordinated nitrocefin, which is almost entirely bound in the presence of an excess of the catalyst. Fits of the experimental data in Figure 6 to the Eyring equation yielded $\Delta H^{\ddagger}$ and $\Delta S^{\ddagger}$ values of 77.6 ± 8.0 kJ mol^{-1} and -62.7 ± 20.0 J mol^{-1} K^{-1}, respectively, for formation of **2′**. The relatively small magnitude of the latter value is consistent with the intramolecular mechanism of Schemes S1 and S2. The negative sign of $\Delta S^{\ddagger}$ suggests that nucleophilic attack is the rate-limiting step; the C−N bond cleavage that follows is fast. The value of the activation entropy is consistent with, but does not entirely prove, the proposed mechanism.

Mechanism of Nitrocefin Hydrolysis by the Dizinc(II) Complex. A detailed mechanism of the $[Zn_2L_1(\mu\text{-}NO_3)(NO_3)_2]$-catalyzed hydrolysis of nitrocefin consistent with the previously published and foregoing results is displayed in Scheme 3. The first step is coordination of the β-lactam carboxylate group to one of the zinc(II) ions. The rate-limiting attack of the bridging hydroxide at the coordinated substrate is followed by fast C−N bond cleavage and formation of **2′**. Protonation of the intermediate upon addition of acid results in release of the product. Nucleophilic attack by a terminal hydroxide in $[Zn_2L_1(\mu\text{-}OH)(H_2O)_2]^{2+}$ can be ruled out because the kinetically important pK_a value of 7.5 is too low to correspond to deprotonation of the terminal water ligand, for which the pK_a is 11.35.[21] This mechanism for the model system agrees well with that proposed for the enzyme.[14,16] The possibility of shifting the attacking hydroxide ion from a bridging to a terminal position prior to its nucleophilic attack at the coordinated substrate also exists.[20,21] The pK_a value for such a shifted hydroxide is expected to be greater than 8.0 because the coordination sphere of zinc(II) contains a negatively charged phenolate ligand.[21] It is therefore unlikely that such a hydroxide shift takes place in the model system. The negative $\Delta S^{\ddagger}$ value seems to support this conclusion. We cannot exclude the possibility of a hydroxide shift in the enzyme mechanism, however.

The presence of potential zinc(II) ligands, such as acetate and 1-methylimidazole, does not significantly affect the decomposition of **2′**. Thus, the concentration of the blue intermediate did not decrease when 0.06 M sodium acetate and 0.005 M 1-methylimidazole were added to the reaction mixture. Only the addition of 0.01 M bpta, a tridentate ligand, resulted in a 15% decomposition of the blue intermediate. Clearly, the nitrocefin fragment in **2′** is strongly bound to the dinuclear zinc(II) complex, consistent with the proposed tridentate structure in Scheme 3 and **2′**.

The presence of zinc(II) complexes clearly stabilizes **2′**. This stabilization, however, is not indefinite, and the blue species decomposed within a day at room temperature.[27,28] Therefore,

Scheme 3

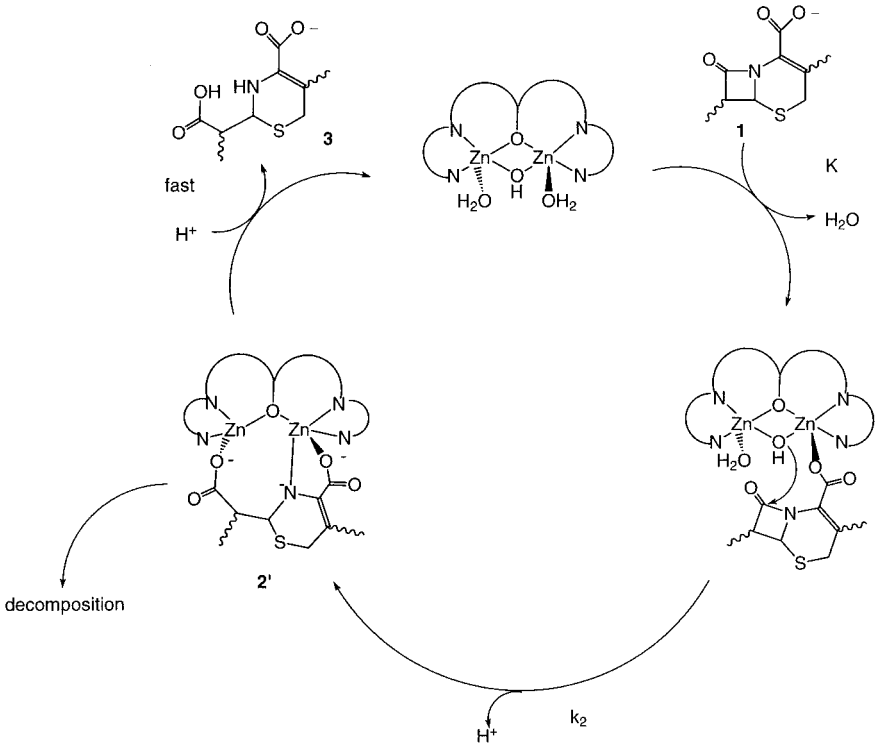

Scheme 4

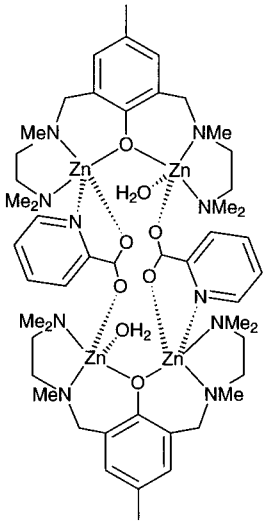

despite much effort, **2′** could not be crystallized. Analogues of the blue species, such as picolinate, are quite stable, however, and studies of their binding to the zinc(II) complexes might shed some light on the structure of **2′**. One such complex, $\{[Zn_2L_1(\text{picolinate})(OH_2)](ClO_4)_2\}_2$, was crystallized, as described in the Supporting Information. The relevant crystallographic parameters are given in Tables S1−S4, and the three-dimensional structure is shown in Scheme 4 and Figure S6. Two picolinates bridge two $[Zn_2L_1(OH_2)]$ units, forming a centrosymmetric dimer. Each picolinate chelates to one of the zinc(II) ions via the pyridine nitrogen and carboxylate oxygen atoms and uses the remaining oxygen atom to coordinate to the other zinc(II) ion. It is likely that hydrolyzed deprotonated nitrocefin **2′** will coordinate to one Zn(II) of the dizinc(II) complex in a similar manner, using its amine nitrogen and carboxylate (C(1)OO) oxygen atoms for binding. The newly formed carboxylate (C(4)OO) is likely to coordinate to the remaining Zn(II) atom. This conclusion is in agreement with the IR and NMR spectroscopic data for **2′**.

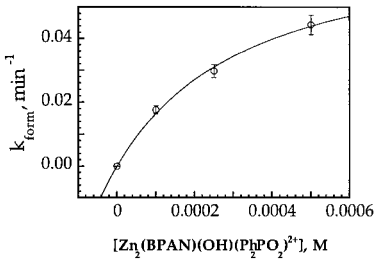

Figure 7. Effect of $[Zn_2(BPAN)(\mu\text{-}OH)(\mu\text{-}O_2PPh_2)](ClO_4)_2$ on the formation of the blue species. The initial concentration of nitrocefin was 3.8×10^{-5} M, the solvent was DMSO, and the temperature was 333 K.

Formation and Disappearance of the Blue Species in the Presence of $[Zn_2(BPAN)(\mu\text{-}OH)(\mu\text{-}O_2PPh_2)](ClO_4)_2$. Mixing nitrocefin and $[Zn_2(BPAN)(\mu\text{-}OH)(\mu\text{-}O_2PPh_2)](ClO_4)_2$ in DMSO solution results in the formation of the blue species, as revealed by its prominent absorbance maximum at 630 nm. Raising the concentration of this complex results in more rapid formation of the blue species (Figure 7). The observed saturation curve arises from binding of nitrocefin to the dizinc(II) complex prior to hydrolysis (Scheme 2B). Fitting the experimental results to eq 4 yielded the respective K and k_2 values of 2810 M^{-1} and 0.075 min^{-1}, lower than the corresponding values for $[Zn_2L_1(\mu\text{-}NO_3)(NO_3)_2]$. The disappearance rate constant k_{dis} is independent of the concentration of the dizinc(II) complex, as revealed by the data in Figure S7.

Formation of the Blue Species in the Absence of Zinc(II) Compounds. One equivalent of base is needed to neutralize the free acid nitrocefin, and therefore, hydrolysis and formation of the blue species are not observed in the presence of an equimolar concentration of $(CH_3)_4NOH\cdot 5H_2O$. Upon addition of a 5-fold molar excess of $(CH_3)_4NOH\cdot 5H_2O$, a blue species at 680 nm was formed almost instantaneously (Figure S8). The predominant product in this reaction, however, was hydrolyzed

nitrocefin (**3**), which has an absorbance maximum at 520 nm. Slight differences in spectral maxima for **3** in these and other experiments presumably arise from variations in reaction conditions.[16] Heating this reaction mixture at 333 K for 1 h resulted in a complete conversion of the blue compound to hydrolyzed nitrocefin **3**. Formation of a blue species and hydrolysis of nitrocefin were not observed in dry DMSO solutions. Clearly, the presence of zinc(II) complexes affords considerable stabilization of **2′**.

Conclusions

Model studies presented here shed light on the mechanism of metallo-β-lactamases. An intermediate **2′** forms in DMSO solutions during nitrocefin hydrolysis; this is the first report of the hydrolytic intermediate that forms in a dizinc(II) model system. Notably, the UV−visible spectra of this species are nearly identical to those of intermediate **2** that was observed in the course of metallo-β-lactamase-catalyzed hydrolysis of nitrocefin.[14] The intermediate was studied in the model system by various spectroscopic and kinetics methods. Carbon-13 NMR and IR spectral data support the proposed structure **2′**. These findings point to a hydrolytic mechanism that involves nucleophilic attack by zinc(II)-bound hydroxide, followed by the C−N bond cleavage (Scheme 3). Protonation of the intermediate affords the products.

Acknowledgment. This work was supported under the Merck/MIT Collaboration Program. B.S. thanks the Swiss National Science Foundation for postdoctoral support. We are indebted to Professor N. M. Kostić of Iowa State University for allowing access to his laboratory facilities to perform some of the UV−visible experiments. We also thank Mr. D. Klein (Iowa State University) for the sample of pyridinium triflate.

Supporting Information Available: Details on the synthesis of $\{[Zn_2L_1(picolinate)(OH_2)](ClO_4)_2\}_2$; Tables S1−S4, showing crystallographic information on $\{[Zn_2L_1(picolinate)(OH_2)](ClO_4)_2\}_2$; Schemes S1 and S2, showing two hydrolytic mechanisms; and Figures S1−S8, displaying absorbances of nitrocefin in the presence and absence of $Zn(ClO_4)_2$, correlation between absorbances of **2′** and nitrocefin, formation and disappearance of the blue species, nitrocefin hydrolysis followed by UV−visible spectrophotometry, UV−visible spectra of **2′** in DMSO solution, an ORTEP diagram and numbering scheme of the picolinate complex, effect of $[Zn_2(BPAN)(\mu\text{-}OH)(\mu\text{-}O_2PPh_2)](ClO_4)_2$ on k_{dis}, and UV−visible spectrum of the blue species in the absence of the complexes, respectively (PDF). X-ray crystallographic data, in CIF format, are also available. This material is available free of charge via the Internet at http://pubs.acs.org.

JA002699E